INNOVATIVE ENERGY CONVERSION SCHEMES FOR SPACE BASED STRATEGIC DEFENSE SYSTEMS

Principal Investigator
Martin I. Hoffert

FINAL REPORT

NYU/DAS 88-001

JANUARY 1988

NEW YORK UNIVERSITY

FACULTY OF ARTS AND SCIENCE

DEPARTMENT OF APPLIED SCIENCE

Accession Number: 4381

Publication Date: Jan 01, 1988

Title: Innovative Energy Conversion Schemes for Space Based Strategic Defense Systems

Personal Author: Hoffert, M. I.

Corporate Author Or Publisher: Dept. of Applied Science, NYU, 23-36 Stuyvesant St., NY, NY 10003
Report Number: NYU/DAS 88-001

Report Prepared for: SDIO, Office of Innovative Science and Technology

Comments on Document: Final Report

Descriptors, Keywords: Energy Conversion Space Based Strategic Defense System

Pages: 00026

Cataloged Date: Mar 15, 1993

Contract Number: DAAL02-86-K-0116

Document Type: HC

Number of Copies In Library: 000001

Record ID: 26438

INNOVATIVE ENERGY CONVERSION SCHEMES FOR SPACE BASED STRATEGIC DEFENSE SYSTEMS

Principal Investigator
Martin I. Hoffert

FINAL REPORT

NYU/DAS 88-001

JANUARY 1988

This research was sponsored by the Strategic Defense Initiative Organization, Office of Innovative Science and Technology, Washington, D.C., under contract DAAL02-86-K-0116 and managed by the Harry Diamond Laboratories.

NEW YORK UNIVERSITY

FACULTY OF ARTS AND SCIENCE

DEPARTMENT OF APPLIED SCIENCE

Innovative Energy Conversion Schemes for Space-Based Strategic Defense Systems

NYU/DAS 88-001

Annual Progress Report for the Period
1 January 1987 - 31 December 1987

Work performed under:
Contract No. DAAL02-86-K-0116

for
Strategic Defense Initiative Organization
Office of Innovative Science and Technology and managed by Harry Diamond Laboratories.

by

Department of Applied Science
New York University
26-36 Stuyvesant Street
New York, NY 10003

Principal Investigator
Martin I. Hoffert

January 1988

TABLE OF CONTENTS

1 INTRODUCTION

A major objective of the Strategic Defense Initiative research program is the development of technologies capable of destroying fleets of ICBM's in the boost phase of their mission by directed energy weapons, perhaps based on a constellation of orbiting satellites or Battle Stations[1,2,3,4]. A strategic defense system may therefore be viewed as a series of energy-conversion steps terminating in the deposition of a "lethal" energy flux on ballistic targets above the sensible atmosphere, together with an information-handling system for tracking, aiming and firing at these targets.

Although these are stringent requirements, a number of potentially effective strategic defense concepts are under evaluation employing fleets of satellites at 200-1000 km altitudes in near-polar orbits. Baseline power requirements for these satellites which have been cited[4] are continuous onboard power at the 100 kW level, and intermittent power at the 10-1000 MW level for perhaps tens of seconds when directed energy devices are energized (Fig.1).

Despite their high power requirements, chemical energy sources for directed energy bursts appear feasible because the durations are short. But the more prosaic 100 kW level housekeeping power cannot be generated chemically for durations longer than a few days without unacceptably large mass to orbit, or unless the fuel is regenerated by an external energy source.

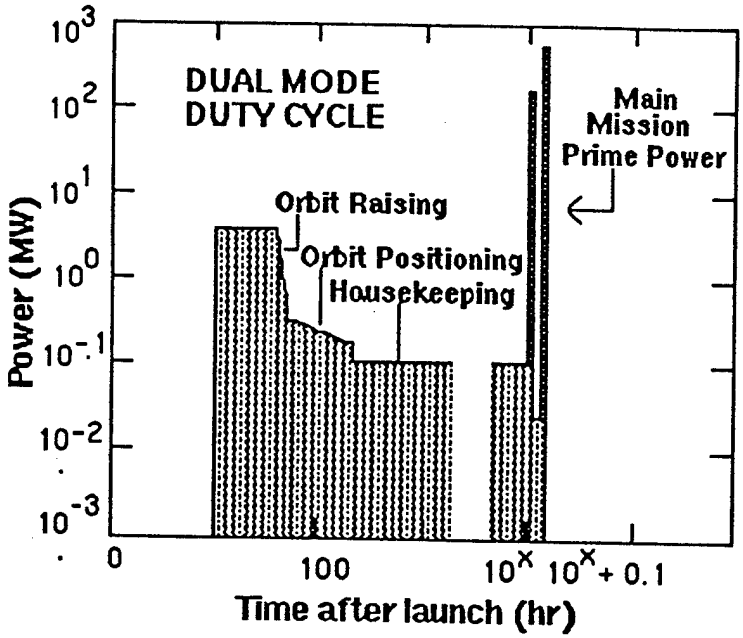

Figure 1. Duty cycle for SDI applications. Satellite platforms will require continuous housekeeping power at the 100 kW (0.1 MW) level and "burst mode" power of 10-1000 MW for tens of seconds over ~ 100 s periods. Power up to the MW level may also be needed for orbital maneuvering.

The frontrunning SDI technology for housekeeping is the nuclear-fueled SP-100 -- a hundredfold scale-up of Uranium-fueled Radioisotope Thermoelectric Generator's (RTG's) flown thus far in space by the US and USSR[5]. However, concern about operational safety problems of RTGs has grown since the Soviet Cosmos 954 satellite malfunctioned in 1977 and spread nuclear debris over a large area of northern Canada[6]. An accidental release of radioactive materials either during launch or on inadvertent re-entry could be quite serious, and has the potential to derail the SDI program in the same way that the Space Shuttle Challenger explosion affected NASA's space program. The developers of the SP-100 are quite aware of these safety issues, and have addressed them in part by designing a reactor which does not go critical prior to orbital status[5]. But

the problem of accidental reentry remains. (Soviet failures may already have caused as many as six nuclear powered satellites to fall back to Earth despite mission profiles designed to put them safely in non-decaying orbits above 500 km altitude.) Current nuclear fueled RTG's at the 1 kW level are thought to contain some 50 kg of Uranium 235 (Ref. 6). Thus simple scale-up to 100 kW implies thousands of kilograms of ^{235}U per space platform, whereas current SDI scenarios indicate hundreds of platforms may be needed for a space-based defensive system[4]. Even if breeder reactors are utilized, large quantities of U-235 will be necessary In commenting on the recent American Physical Society (APS) Report on directed energy weapons in space (Ref. 4), the New York Times (April 23, 1987) said"...one key conclusion of that is bound to increase political opposition to an anti missile defense (is that) many space-based platforms would require reactors for power, thereby undercutting assertions that the defensive system would be entirely non-nuclear". It is therefore reasonable to ask whether an entirely non-nuclear system for all power modes of SDI satellites is feasible.

We are proposing an entirely non-nuclear microwave beam power supply for orbiting spacecraft which addresses SDI power requirements, uses technology near the state-of-art, and can be developed and tested relatively inexpensively in proof-of-concept experiments over a period of 3-5 years. These beams would provide high power transmissions over intermittent periods when the satellite is in a line-of-sight from the ground. The energy is stored chemically for later use.

The idea of beaming microwave power over long distances in space has been studied thus far primarily in connection with the Solar Power Satellite (SPS) -- a large photovoltaic solar array in geostationary orbit beaming microwave energy through the atmosphere to a rectifying antenna (rectenna) at the Earth's surface for distribution by an electric power grid[7,8,9,10,11]. Related ideas are microwave reflector satellites to relay power between points on the Earth[12,13,14] and microwave transmissions to provide power to spacecraft[15,16]. For the present application, the APS Panel[4] suggested that SDI satellites might be powered by a system of microwave relay satellites. We considered this idea, but believe excessive beam diffraction and steering problems over thousands of kilometers along with the complexities of maintaining continuous transmissions could be a problem. It is possible that the system proposed here could evolve in time to one in which prime power is generated by geostationary solar power satellites, as opposed to the Earth's surface, and subsequently beamed to satellites in Low Earth Orbit (LEO). However, the infrastructure of space operations needed and the large capital investment to build a SPS would seem to defer this system some decades into the future.

Our scheme, Microwave power to Low Earth Orbit (MTL) has the virtue of being a near term technology. It requires six steps, all of which have been accomplished individually to some degree in the laboratory or field: (1) generate the primary electrical power (DC) at ground-based stations by conventional nuclear or fossil fuel plants; (2) convert this DC to RF (microwave) frequencies using microwave generators; (3) transmit RF power in a narrow beam to the spacecraft using phased array antennas to track and lock-onto satellites as they pass in range during a fraction of their orbits; (4) receive and convert the RF to DC power in space with lightweight and inexpensive rectennas; (5) store the electrical energy chemically by electrolysis of water or steam to hydrogen and oxygen and (6) recover the free energy of the hydrogen and oxygen gases onboard the spacecraft during the balance of the orbit as continuous DC (or on demand) to a load with high power-density fuel cells.Its advantages can be summarized as follows:

- ⊕ Space-based components are entirely non nuclear
- ⊕ Space-based components are solid state and gases, have few moving parts and produce no effluents
- ⊕ Heavy primary power remains on Earth -- low mass-to-orbit
- ⊕ Phased-Array Transmitting Antenna is steerable over a range of scan angles from zenith
- ⊕ Transmitting antennas at a few sites can recharge hundreds of satellites
- ⊕ Rectenna is low mass, low cost etched circuit technology
- ⊕ Thermal dissipation and microwave collection functions can be integrated in rectenna design
- ⊕ Storage system provides energy when and where needed in orbit
- ⊕ Solid oxide regenerative fuel cells have potential for veryhigh power densities -- low mass-to-orbit
- ⊕ Regenerative fuel cell can supply both housekeeping and burst mode power

2. COMPARISON WITH OTHER SPACE POWER SYSTEMS

Energy sources usually discussed for Space Power applications are nuclear, chemical and solar. In assessing any prime power source for a given space mission it is necessary to consider a number of factors: its energy per unit mass (specific energy), its ability to supply power per unit mass (specific power), the required duration of use, the possibility of utilizing components for multiple applications, overall system reliability and cost. The environmental safety of nuclear power systems onboard spacecraft, particularly when a large constellation of platforms in relatively low orbits is involved, must also be considered, and may be decisive for operational systems. Indeed, it is through a consideration of the interplay of all these factors that the advantage of MTL emerges.

In light of high launch costs per unit mass, the most elementary consideration for space power systems is their specific energy. This quantity depends ultimately on the storage capacity of nuclear, electromagnetic (chemical), gravitational and inertial states of matter, and ranges over astronomical orders of magnitude for practical systems (Table 1)

Nuclear power systems are not normally considered to be fuel mass limited over the mission times of interest, while solar power employs massless photons whose flux is limited by the solar constant. The availability of power from stored chemical energy depends critically on the duration of use. The specific power of all systems can be limited by the mass of the energy-converter, and the ability of current technology to scale-up converters to needed levels. Clearly, the mass of nuclear fuels needed is much less than that of the chemical (H_2/O_2) fuels proposed for MTL as onboard energy buffers for a given total energy drain. But nuclear fuels are not be easily regenerated. For housekeeping, they must provide energy continuously over a 10 yr satellite lifetime whereas chemical fuel cells can be recharged by microwave power from the ground.

Table 1. Specific energy storage of various materials and systems in kJ/kg (Ref. 17). The theoretical maximum specific energy for matter/antimatter conversion to pure energy is $c^2 \approx 9 \times 10^{13}$ kJ kg^{-1}

Deuterium (D-D fusion reaction)	$3.5X10^{11}$	Silver oxide-zinc battery	437
Uranium-235 (fission reaction)	$7.0x10^{10}$	Lead-acid battery	119
Heavy water (fusion reaction)	$3.5x10^{10}$	Flywheel (uniformly-stressed disk)	79
Reactor fuel (2.5% enriched UO_2)	$1.5x10^{9}$	Compressed gas (spherical container)	71
Natural uranium	$5.0x10^{8}$	Flywheel (cylindrical)	76
95% Pa-210 (radioactive decay)	$2.5x10^{6}$	Organic elastomer	20
80% Pu-238 (radioactive decay)	$1.8x10^{6}$	Flywheel (rim-arm)	7
Hydrogen (Lower Heating Value)	$1.2x10^{5}$	Torsion spring	0.24
Methane (Lower Heating Value)	$5.0x10^{4}$	Coil Spring	0.16
Gasoline (Lower Heating Value)	$4.4x10^{4}$	Capacitor	0.016
Lithium hydride (@ 700°C	$3.8x10^{3}$		
Falling water (Δz = 100m)	$9.8x10^{2}$		

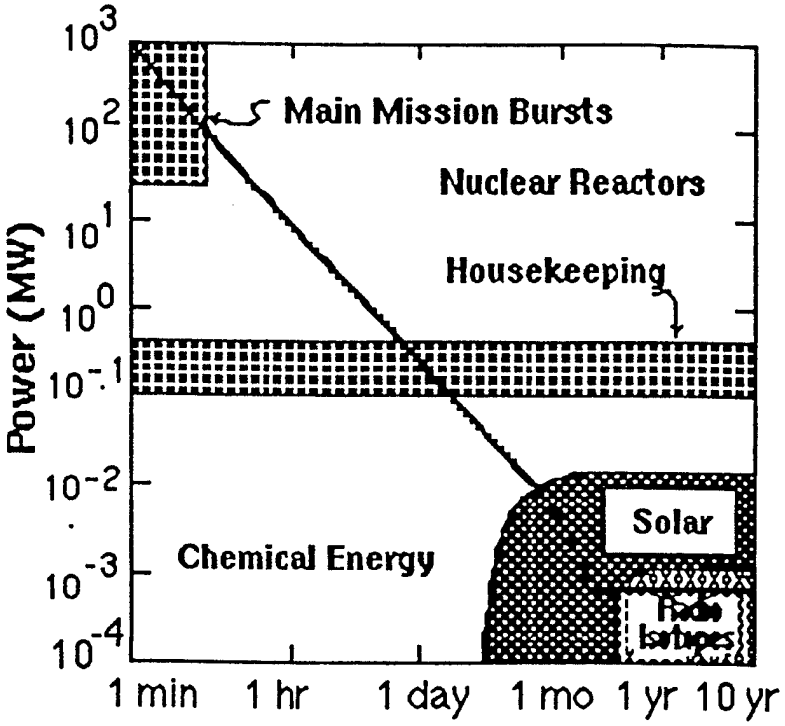

Figure 2. Comparison of electrical power requirements versus duration for housekeeping and burst mode applications with conventional space power energy sources (Ref. 4).

The breakpoint between chemical and nuclear power systems in Fig. 2 is a function of duration. For example, at the housekeeping level (100 kW = 0.1 MW) chemical energy sources are nominally presumed to be exhausted after about 1 day ($\sim 10^5$ s), corresponding to a total energy of $\sim 10^7$ kJ. Because of the oxidizer mass, the theoretical specific energy of a stoichiometric hydrogen/oxygen mixture is 1/9 the heating value of molecular hydrogen, or $\sim 10^4$ kJ kg^{-1} from the Table 1 value for H_2. For example, $\sim$ 1000 kg day^{-1} of fuel/oxidizer mixture is needed to produce 100 kW if a 100% efficient hydrogen/oxygen fuel cell were used to generate onboard electricity, whereas as comparable mass of Uranium could power the satellite at this level for its entire lifetime. These order of magnitude arguments underlie the conventional wisdom that nuclear sources are needed for SDI housekeeping.

We are proposing however to reverse the fuel cell to a electrolysis cell while the satellite is energized by microwaves, thereby regenerating H_2 and O_2 from the steam product periodically. The recharge frequency needed depends on the efficiency of the electrochemical cell and on the allowable mass of buffer gases carried onboard, but should be of the order of days or less. In that case the onboard fuel mass for nuclear reactors and for MTL energy are comparable, while the use of chemical energy in orbit has the advantage of avoiding the nuclear safety issue. (Possible objections to microwave beam propagation through the atmosphere on environmental grounds were extensively studied during the NASA/DOE SPS program and were found to be relatively insignificant for the beam flux densities proposed here[9]).

Alternately, the $\sim 10^{10}$ J of chemical energy in each tonne (1000 kg) of reactants could produce 10^8 W (100 MW) if reacted over a period of 100 s. This is the power level and duration of the burst mode. Similar considerations suggest orbital changes could also be accomplished within this range of total energy. There is therefore the possibility with MTL of developing a multi mode power supply for housekeeping, orbit maneuvering and burst modes using common components, and requiring an onboard inventory only of the order of tonnes of chemical fuel . This is a minor fraction, for example, of the Space Shuttle payload capacity ($\sim$ 30 tonnes for orbital injection to LEO[18,19]).

In solar-powered space systems the energy and transmission systems are "free". But there are other problems: In assessments of the solar photovoltaic option it must be borne in mind that with the possible exception of satellites in GEO or higher orbits, geometric considerations dictate that a fraction of the orbit is spent in the Earth's shadow. Photovoltaic systems must therefore either use their energy continuously, or, when used for satellites in LEO which spend some of their time in the Earth's shadow, must store it for use on demand. They are further constrained by the energy flux available from the sun (solar constant), $S_0 \approx 1.36$ kW m^{-2}, by costs, and by their band-gap energy, which in combination with the solar spectrum limits them to theoretical peak efficiencies of ~ 35 % and practical peak efficiencies of 10-20%. Solar cells are also potentially more vulnerable to radiation damage than the rectennas of MTL. Solar thermodynamic cycle efficiencies may be in the 30-40% range, depending on operating temperature, but require heat engines with moving parts to extract electrical power.

Figure 3 shows an early NASA Space Station Reference Design with a solar collector area A $\approx$ 1780 m^2 producing a mean busbar power/orbit for the manned habitat core at 500 km altitude of P $\approx$ 75-300 kW (Ref. 20). This is also the continuous power range needed for SDI housekeeping. The overall efficiency of this system is relatively low, $\eta = P/S_0A \approx$ 3-12%, which includes the effect of spending part of the orbital period in the Earth's shadow. Figure 3 also shows the MTL concept applied to a hypothetical Laser Defense Station.

During its entire orbital period, the structural framework of orthogonal beams of the Space Station maintains a fixed orientation relative to the Earth's surface. This attitude is gravity-gradient stabilized with the Shuttle docking port earthward. More recent design have the habitats moved to the platform's center of mass to facilitate microgravity experiments, but gravity-gradient stabilization of the main structure remains an essential feature. One consequence of this is that the photovoltaic array panels must be actively rotated around the horizontal and vertical axes of the crossed beams to capture the maximum component of incident solar flux. Indeed, continuous two-axis sun tracking is needed by any solar powered satellite in LEO that maintains a fixed orientation relative to the Earth's surface to prevent efficiency from dropping to even lower, and economically unacceptable, values.

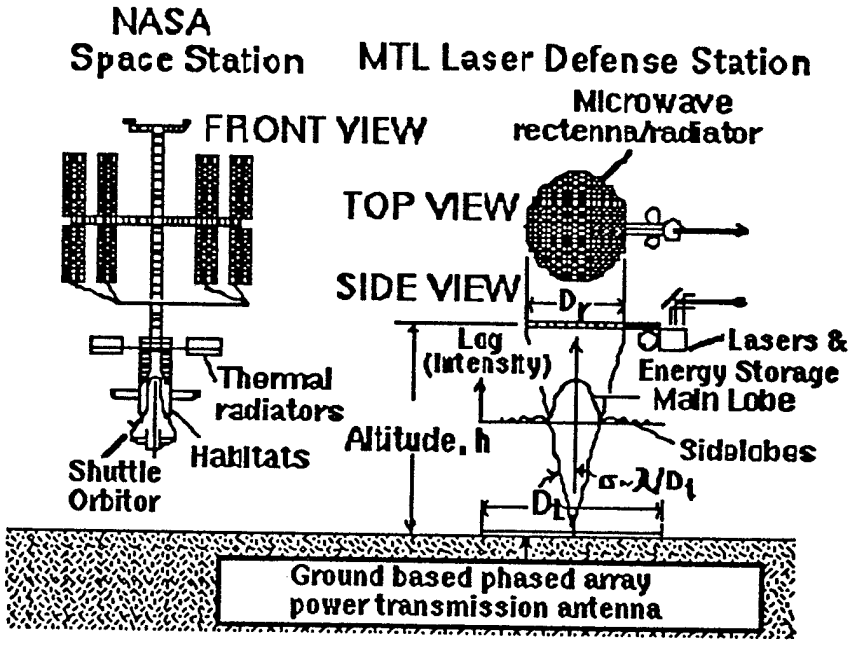

Figure 3. **An early (1984) NASA Space Station design (LEFT) powered by photovoltaic cells with 75-300 kW DC mean output is compared with the Microwave power To Low Earth Orbit (MTL) concept. The application of MTL to SDI systems proposed here (RIGHT) provides a constellation of defensive satellites with continuous housekeeping at the 100 kW level.**

Control of the rectenna orientation relative to the transmitter is also needed for MTL power. We considered rotating the rectenna around a horizontal axis normal to the flight path as it overflies the transmitter such that the receiving plane remains normal to the transmitted beam axis, but have opted instead for a horizontal orientation. A crude scaling is that incident power is proportional to $\cos^2\Theta_0$ for a rotated rectenna and $\cos^3\Theta_0$ for a horizontal one, where Θ_0 is the scan angle from zenith. The advantage of rotation is much less than for the solar panels, whose incident flux scales with the cosine of the off-normal incidence angle, because of the strong dependence of the normal component of microwave radiation at the rectenna on distance from the transmitter -- the variation in distance from the sun is negligible for Earth-orbiting solar panels. This is fortunate since there are important factors motivating a horizontal rectenna. We envision that the backplane of the rectenna will function as a thermal radiator dissipating energy produced onboard to space. The surface area is close to the value needed for this function alone. A flat horizontal rectenna presents the minimum frontal cross section to orbital debris, perhaps orders of magnitude below what a sun-tracking photovoltaic array would display. Since an adversary might intentionally introduce counterorbiting pellet clouds as countermeasures against satellite platforms[4], the decreased vulnerability associated with a low frontal area horizontal orientation is a distinct advantage.

3. ORBITAL CONSIDERATIONS

Constraints on orbital altitude of space-based ballistic missile defense systems are derived in Refs. 4, 21 and 22. Let H (J m^{-2}) be the "hardness" of the boosters to be destroyed, B (W sr^{-1}) the brightness of the space-based beam weapon, and $k \equiv H/B$ (s m^{-2}). The number of satellite platforms per unit area s needed to destroy an attack by uniformly distributed boosters per unit area b depends mainly on the duration of boost phase t_B, the retargeting time of the weapon t_T, and the orbital altitude h. The satellite altitude appears in the formulation though its influence on the "effective" retargeting time, $t_T' \equiv t_T + kh^2$. The satellite and booster areal densities are related in the uniformly distributed case by (Ref. 4; Appendix B):

$$s = \frac{b}{2}\left\{\frac{t_T}{t_B}\right\}\left\{1+\sqrt{1+\frac{b^*}{b}}\right\},$$

where

$$b^* = \frac{2}{\pi}\left\{\frac{t_B}{t_T'}\right\}\left\{\frac{k}{t_T'}\right\}\left\{\frac{R_e}{R_e+h}\right\}.$$

The total number of satellite platforms uniformly distributed over a spherical shell at altitude h is then given by $N_{sat} = s \cdot 4\pi(R_e + h)^2$, where $R_e = 6.37\times10^6$ m is the Earth's radius. To find the altitude dependence of N_{sat}, we choose nominal values of the parameters within the range normally cited: H = 200 MJ m^{-2}, t_B = 200 s, t_T = 0.1 s and b = 1.4×10^{-10} boosters m^{-2} [This booster density is based on distributing the current inventory of 1400 Soviet boosters over the current Soviet deployment area of ~ 10 $(Mm)^2$]. In Table 2, we show number of satellites needed as a function of altitude between 200-1000 km for a nominal laser brightness of $B_0 = 2.69\times10^{20}$ W sr^{-2} and for a brightness an order of magnitude higher.

Table 2. Number of defensive satellites required as a function of altitude for nominal parameter values and for a high brightness laser. A tenfold increase in laser brightness could be attained with the same level of burst mode power if the wavelength could be decreased by $\sqrt{10}$ with no loss of efficiency (Ref. 22).

Altitude (km)	No. of Satellites $B = B_0$	$B = 10 \times B_0$
200	180	72
300	193	75
400	211	78
500	234	82
600	264	87
700	302	92
800	349	98
900	405	105
1000	473	113

The main message of these results is that more satellites are needed when the constellation is at a higher average orbital altitude, although the altitude dependence is weaker for brighter weapons. Clearly, satellite costs to some extent drive the system to lower altitudes, whereas safety considerations of onboard nuclear reactors drive it higher. Energy losses by atmospheric drag (which must be actively corrected to prevent orbital decay), and vulnerability issues, may also drive the system to higher altitudes or at least limit the minimum altitude. The optimum orbits are by no means obvious at this time, and are strongly influenced by booster burn time and retargeting times. In addition, the following MTL system requirements need to be considered in an orbital trade-off:

⊕ Satellites should be along paths which at least daily pass within range of microwave power transmission sites and perhaps other specified points on the rotating Earth.

⊕ Satellites should be in view of one or more ground based power stations for a sufficient fraction of of their orbits to deliver the power required for operational modes (with energy storage).

⊕ This power should be deliverable at acceptable efficiencies to rectennas of reasonable size.

⊕ Incident power intensities should be below electrical and thermal overload limits of rectenna elements (diodes are limiting).

⊕ Vulnerability should be minimized at the preferred low altitudes

⊕ Satellites should have maneuvering capability for attitude control and for orbital altitude changes needed during mission.

⊕ Orbital paths may be constrained by conditions related to system requirements, which may lead to satellites in a number of different orbits (different altitudes and orbital inclinations).

In what follows, we establish orbital considerations independent of the last trade-off listed. It is understood that mission requirements may preclude the scenario depicted herein. From a reception viewpoint the most essential requirements are that satellites be accessible to recharges from surface transmitting antennas sufficiently frequently, and for appropriate periods of time, to minimize the onboard mass of electrochemical cell reactants used as energy buffers for the balance of the orbit. In our specific reference system developed later, phased array transmitting antennae electronically track satellites in near polar orbits in both azimuth and zenith angle, and focus power on rectennas as they fly across a high-latitude "picket fence". It is worth recognizing however that a simplification of the transmitter design with potential cost advantages might be possible if transmitters need only be steered around one axis. As discussed next, this might be achievable if the satellites were in overlapping orbits.

The accessibility of spacecraft to transmissions from the surface depends on the orbital plane and orbital period. The period of a circular satellite orbit is[23]:

$$T_S(h) = \frac{2\pi(R+h)^{3/2}}{g_o^{1/2}R},$$

where $g_o = 9.81$ m s^{-2} is gravitational acceleration at the surface. Thus a satellite at h $\approx$ 500 km has a period $T_S \approx 6100$ s (102 min). The period increases with altitude such that it becomes geosynchronous with the Earth's rotation at h $\approx$ 35800 km. A geosynchronous orbit is in the equatorial plane is also geostationary -- it maintains a fixed orientation relative to a point on the surface -- otherwise its ground track oscillates over a repetitive path. There are also "quantized" orbits below the geostationary altitude, with periods of an integral fraction of a sidereal day, which follow repeating paths on the rotating Earth below them. Because these orbits overlap it may be possible to build transmitters along their ground path which need track around the zenith axis only. The discrete altitudes of quantized circular orbits for a spherical Earth are given in Table 3. Orbits at $\approx$ 270 and 560 km altitude may allow simple one axis tracking for missions where is not necessary to fly satellite constellations at arbitrary altitudes for other reasons. Polar orbits are desirable for SDI or remote sensing missions since they allow platforms to pass over high latitudes of both hemispheres. Because of the convergence of meridians it is desirable to place ground stations near the pole, even for nonoverlapping orbits, since satellites in highly inclined orbits are accessible to transmissions with a fewer number of ground stations.

Atmospheric drag imposes a lower limit on orbital altitude in the vicinity of 200 km, although the MTL rectenna is expected to have a significantly smaller frontal area, and hence less drag, than satellites powered by sun tracking solar panels. Nonetheless some onboard mass and a fraction of the transmitted energy would have to be expended for attitude, and perhaps altitude, control to keep the satellite in a particular (low) orbit. One result of orbital mechanics is that atmospheric drag causes large reductions in the apoapsis of satellites in elliptical orbit, so that low altitude orbits become circular, whether by design or not[23]. The availability of significant levels of onboard electrical power would permit the use of high specific impulse ion propulsion for orbital maneuvers, including the orbit raising mode of Fig 1, as opposed to less mass efficient chemical rockets. Brown and Glaser (Ref. 15) have already proposed raising satellites in low equatorial orbits to GEO altitudes using ion thrusters energized by microwave beams from the Earth. However, there is no fundamental reason why orbit raising could not be accomplished using microwave power transmitted to more inclined trajectories.

Table 3. Apparent movement to the West in degrees longitude per orbit and altitude for 16 polar orbits which which overfly a given latitude and longitude once each day. MTL transmitters aligned along the ground track need only scan in zenith angle to access these orbits.

No. orbits per day	Deg. long per orbit	Altitude (km)	No. orbits per day	Deg. long per orbit	Altitude (km)
16.	22.5	267.4	8.	45.0	4166.3
15.	24.0	559.3	7.	51.4	5147.2
14.	25.7	885.4	6.	60.0	6393.8
13.	27.7	1252.9	5.	72.0	8043.4
12.	30.0	1670.7	4.	90.0	10355.3
11.	32.7	2150.9	3.	120.0	13891.3
10.	36.0	2709.9	2.	180.0	20179.8
9.	40.0	3370.6	1.	360.0	35775.1

4. TRANSMITTER AND RECTENNA TECHNOLOGY

The implementation of MTL in hardware should not require technological breakthroughs so much as dedicated systems engineering and application of existing microwave technology. For a given orbital scenario, the key parameter influencing microwave power system selection is probably the operating frequency; $\nu \equiv c/\lambda$, where λ is the wavelength. The microwave power sources for the phased array transmitter as well as the geometry of transmitting and receiving antennas are all impacted by this choice. Some hardware considerations linked to frequency which have emerged in our study thus far are discussed below.

An overriding consideration in the feasibility of the MTL and of the earlier SPS concept is the relatively transparency of the atmosphere to microwave frequencies, even in the presence of clouds. Propagation losses through the atmosphere should be small, but not altogether avoidable at certain frequencies. Scattering from molecules, cloud condensation nuclei and hydrometeors is frequency-dependent. But unless it is raining, the atmosphere is > 90% transparent over the wavelength window from 1 - 50 cm corresponding to frequencies of 30 - 0.6 GHz (Ref. 24). The main attenuation of transmissions is likely to come from raindrops at the small λ end of the microwave spectrum, with effects depending on the severity of precipitation: At $\lambda \sim 4.2$ cm (7 GHz), 10% of the transmission is lost to scattering by a 5 mm/hr uniform rain, 40% is lost from 50 mm/hr rain; and 90% lost in a severe thunderstorm (Ref. 25, Fig. 2.1). Though episodic, the possibility of precipitation losses drives the system toward $\lambda > 10$ cm wavelengths, where even rain becomes transparent. Direct absorption of the beam by the ionospheric plasma is small at microwave frequencies but refraction and consequent beam displacement may have to be considered[26].

The starting point of the microwave beam launched from the face of the phased array is the microwave generator. We considered various power generating tubes for the DC-to-microwave frequency conversion step, including magnetrons, klystrons, travelling wave tubes (TWTs) and solid state devices. The most promising contender for the high-efficiency continuous operation we seek may be the simple magnetron.

These are envisioned as distributed sources feeding power and steering the beam of a slotted waveguide phased array. Magnetrons are the oldest and best understood of crossed-field microwave electron tubes wherein electrons generated at a heated cathode move under the combined force of a radial electric field and axial magnetic field. Their cylindrical geometry causes electrons to interact synchronously with the travelling wave components of a standing-wave pattern in the cavity such that electric field potential energy is converted to microwave energy at high efficiency. The electron distribution rotates in the cylindrical annulus between an outer anode and a heated inner cathode in a "bunched" fashion -- somewhat like a hub with spokes in solid body rotation at the mean tangential drift velocity (E/B). Thermionically emitted electrons from the cathode are the "spokes" of a wheel rotating at near synchronous velocity in phase with the standing wave. Thus radial direct current is converted to microwave energy. Ceramics are often employed as output windows which separate inner (vacuum) and outer environments to covey microwave power output to the outside world. The dielectric breakdown of these insulating windows often constrains the output power per tube; which is of order 1 kW for frequencies in the 1 - 40 GHz microwave power spectrum. The matching of electron tangential velocities with the standing wave pattern results in relatively high conversion efficiencies of $\eta_M \approx 65$-75%. Thus magnetrons offer fundamental efficiency as well as cost and reliability advantages.

A proposed modification for driving the MTL phased array is to convert a permanent magnet magnetron from a free-running oscillator into a directional amplifier by adding a ferrite circulator as passive directional device[25]. This amplifier is controlled by feedback loops which modify the phase and amplitude of the output signal such that they track phase and amplitude references. Phase control of the output is by a phase comparison between the output and reference signals whereupon an appropriate phase shift is fed back to eliminate the difference. Amplitude control of the output of the magnetron directional amplifier is done by a "buck boost" coil, which adds or subtracts to the residual magnetic field established by permanent magnets. Phase control is needed to maintain the coherence of the transmitted beam while steering and focusing it, and amplitude control is needed to vary output power.

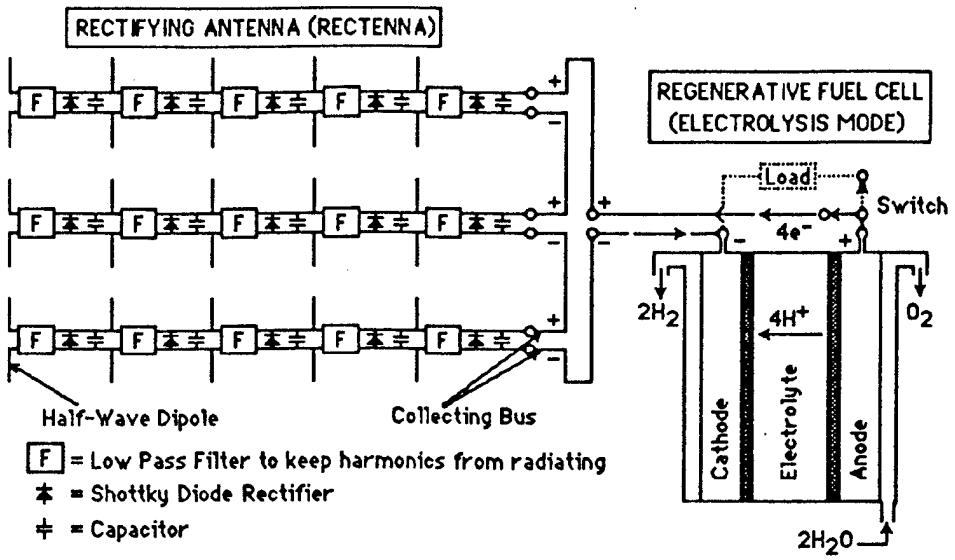

Figure 4. **Schematic diagram of rectenna and regenerative fuel cell in the MTL application. State-of-the-Art rectenna technology developed at the Raytheon Corporation employs a 20 μm Kapton F dielectric film as a substrate on which copper dipoles are deposited. W.C. Brown projects this foreplane bonded to a metallic reflecting plane could be fabricated at area densities as low as 0.170 kg m^{-2} (Ref. 28).**

The physical size of the transmitting antenna and interelement spacing along it are both proportional to wavelength. Shorter wavelengths permit smaller transmitter apertures but do not necessarily reduce the number or cost of radiating components, and have the disadvantage of increasing the heat dissipation per unit area. Similar considerations apply to the receiving antenna, which in addition to antenna elements contains temperature-limited rectifying diodes.

Integrated circuit rectifying antennas can be traced to pioneering work in the 1960's at the Raytheon Corporation, where one was used in a demonstration of a beam-riding microwave power helicopter[27]. At that time W.C. Brown[27] recognized that solid state semiconductor diodes were desirable as microwave rectifying circuit elements since their cost, bulk and impedance (the ratio of output voltage to current) were all relatively low compared to alternatives like inverting microwave power generators (magnetrons, klystrons or TWT's). The technology was subsequently developed during the DOE/NASA SPS Program (now defunct). The potential cost per unit area of this component is an order of magnitude or more below, for example, crystalline photovolatic panels for direct solar power. Unfortunately, the absence of a clear cut application thus far has limited production of this lightweight and inexpensive space power technology to a small scale "cottage industry". This would certainly change if MTL were adopted as a power supply for constellation of SDI satellites. Our rectenna is envisaged as fabricated by thin film etched circuit techniques. The printed circuit includes solid half-wave dipole antenna elements feeding alternating current to solid state Schottky diodes for conversion to direct current. Structural elements needed to maintain the orientation of the rectenna relative to the surface may also be needed, as discussed earlier. Figure 4 illustrates the rectenna array components and power-handling system of collecting busses driving a schematic electrochemical cell during the charging cycle. One feature which needs to be better understood is the power conditioning needed to optimize the energy storage system efficiency over the charge-discharge duty cycle. This power conditioning must provide impedance matching between the rectenna and the electrolysis mode of the electrochemical cell during charging as well as an impedance match between the fuel cell mode and the load during discharge to provide the maximum round trip efficiency.

Apart from the physical constraints of atmospheric absorption and the technological aspects of generating and receiving microwave power there are operational factors driving the system toward certain microwave frequencies: In particular, the 2.45, 5.8 and 24.125 GHz (12.2, 5.1, and 1.24 cm) bands have been assigned and are accepted by international regulatory authorities for industrial, scientific and medical purposes[29]. They have the advantage of not interfering with assigned communication channels and are compatible with existing international treaties and commercial agreements. This could be

important if and when the MTL concept is tested. Moreover, the 2.45 GHz (12 cm) channel was the frequency of choice in previous studies of the Solar Power Satellite (SPS), so many of the technological and environmental issues are well understood.

5. EFFICIENCY OF POWER TRANSMISSIONS TO ORBITING PLATFORMS

For most cases of interest here the rectenna is in the near field of the transmitted beam. For systems reasons we may want to focus radiant energy on an orbiting rectenna which is smaller than the transmitter ($D_r < D_t$ -- the product D_rD_t determines transmission efficiency and it seems easier at this point to build a large transmitter at the surface that to deploy a large receiver in orbit). In the small wavelength limit ($\lambda/D_t \rightarrow 0$) wave propagation is described by geometric optics so a uniformly illuminated spherical antenna of finite aperture would hypothetically focus all the radiant energy on a focal point where $I \rightarrow \infty$ (Figure 5, LEFT). This can be done with a phased array antenna by controlling the phase distribution across the aperture (Figure 5, RIGHT). However the finite wavelength at which the antenna operated creates beam divergence from diffraction which limits the minimum receiver size needed to capture a given fraction of transmitted energy.

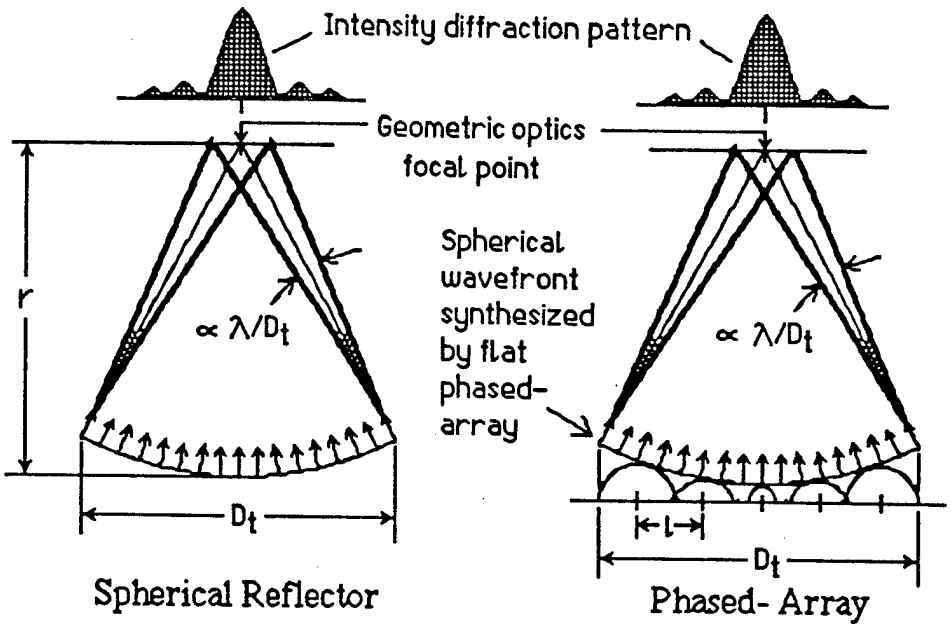

Figure 5. **Converging microwave beam producing peak intensity at focal point and spread by diffraction. (LEFT) Uniformly illuminated spherical reflector; (RIGHT) flat array of radiating elements producing spherical "imploding" wave by phase shifts. In the MTL system both steering and focussing are done electronically by phase shifts.**

The minimum diffraction of a converging microwave beam at the focal point in the near field is equivalent to the "far field" diffraction of a parallel beam expressed as an angular deviation from the center of the transmitting aperture[31]. This diffraction limit is analogous to that of a laser beam emanating from 10 m mirror focussed on a 1 m spot on an ICBM booster thousands of kilometers away. Of course, we want to energize the rectenna, not destroy it, but the diffraction and focussing issues are similar. Our nominal transmitter design is a flat phased array[32]. Other concepts, including arrays of parabolic antennas with Cassegrain feeds and large steerable antennas driven by a central feed employing individually displaced reflecting panels were considered, but at this point the mechanical simplicity of a fully electronic phased array seems most advantageous.

We assume the transmitter is a horizontal square array of side D_t with $N \times N$ isotropically radiating elements uniformly spaced a distance $\ell = D_t/N$ apart. This is an idealization of the slotted waveguide radiation sources we envision as uniformly distributed over the transmitter. A reflecting backplane will probably be necessary to avoid downward power losses.

By varying the input phase distribution across the array, a focussed coherent beam is produced along the boresight r_o which tracks the center of a square rectenna of side D_r.

The incidence angles of rays from the transmitter aperture center on a horizontal plane are related to the zenith and azimuth angles (Θ, ϕ) of the spherical coordinate system by (Fig.6)

$$\sin\Theta_x, \sin\Theta_y = \sin\Theta\cos\phi, \ \sin\Theta\sin\phi .$$
$$\sin\Theta_{xo}, \sin\Theta_{yo} = \sin\Theta_o\cos\phi_o, \ \sin\Theta_o\sin\phi_o .$$

Assuming the phase shifts fed along each axis are independent, the diffraction-limited intensity field normalized to the boresight peak is expressible as the product of the x and y distributions[33,34]:

$$\frac{I}{I_o} = \left\{\frac{E}{E_o}\right\}^2 = \left\{\frac{\sin\frac{N\Psi_x}{2}}{N\sin\frac{\Psi_x}{2}}\right\}^2 \times \left\{\frac{\sin\frac{N\Psi_y}{2}}{N\sin\frac{\Psi_y}{2}}\right\}^2 ,$$

where

$$\Psi_x \equiv k\ell(\sin\Theta\cos\phi - \sin\Theta_o\cos\phi_o) = k\ell(\sin\Theta_x - \sin\Theta_{xo}) \cong k\ell\Delta\Theta_x\cos\Theta_{xo} ,$$
$$\Psi_y \equiv k\ell(\sin\Theta\sin\phi - \sin\Theta_o\sin\phi_o) = k\ell(\sin\Theta_y - \sin\Theta_{yo}) \cong k\ell\Delta\Theta_y\cos\Theta_{yo}$$

Here $k = 2\pi/\lambda$ is the wavenumber, subscript zero denotes the boresight direction, and the approximations are for small angular deviations from r_o. These are the deviations in the xr and yr planes are defined by $(\Delta\Theta_x, \Delta\Theta_y) \equiv (\Theta_x - \Theta_{xo}, \Theta_y - \Theta_{yo})$. It can be shown that $\Delta\Theta_x, \Delta\Theta_y$ are of order $\lambda/D_t << 1$, so the physical displacements normal to the boresight axis are $\approx (r\Delta\Theta_x, r\Delta\Theta_y)$. However a consequence of the oblique projections of the beam when the boresight is at arbitrary incidence, the intensity distributions normal to boresight are elongated over the rectenna face such that $I/I_o(\Delta\Theta_x, \Delta\Theta_y) = I/I_o(x,y)$, where

$$x, y \approx r\Delta\Theta_x/\cos\Theta_{xo}, \ r\Delta\Theta_y/\cos\Theta_{yo}$$

are the coordinates on the horizontal rectenna (Fig. 6).

The apparent inderminacy at the boresight can be evaluated by L'Hospital's rule which gives $I_o/I_o = 1$; a local peak, as expected. However, a major constraint on the number of individual radiation sources N^2 is the avoidance of so-called grating lobes -- off boresight peaks which develop when the numerators of the array pattern functions = 0 anywhere in the semi infinite half-space above the transmitter. To avoid them we need $\Psi_x/2, \Psi_y/2 < \pi$. Since $|\sin\Theta_x - \sin\Theta_{xo}| \leq 2$, this condition requires $\ell < \lambda/2$ ($N > 2D_t/\lambda$). For example, a transmitter of 500 m aperture operating at a 10 cm wavelength needs 10^4 elements per side (10^8 elements for the square array) to prevent power diversion from the boresight direction by grating lobes.

This is obviously a large number of individual radiating elements, but these may be as simple as slots cut into a network of microwave waveguide "plumbing". System costs are more likely to be driven by costs of microwave radiation sources, phase shifters and microprocessors than by radiating elements as such. While high power magnetrons or solid state oscillators could be set up to drive many radiation sources, each radiating element needs to be driven by its own phase shifter to prevent degradation of beam quality as it is focussed and scanned over large angles. The problem is simplified considerably if the beam need be steered over large angles around one axis only, as in the quantized orbits case discussed earlier.

To compute the power incident on the rectenna, we want to recast the idealized intensity pattern with the rectenna coordinates (x,y) as the independent variables.

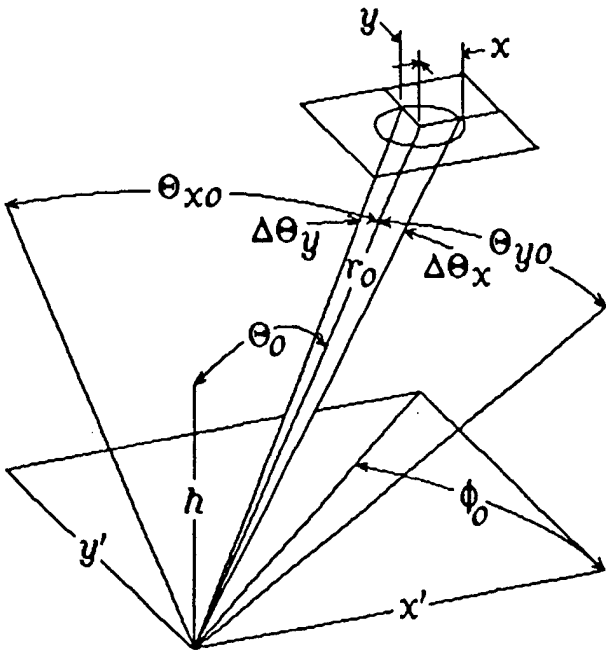

Figure 6. **Geometry of horizontal transmitter and receiver during a flyby. The spherical coordinates r, Θ and ϕ are related to the Cartesian coordinates measured from the center of the transmitter by x' = rsinΘ cosϕ = rsinΘ_x, y' = rsinΘ sinϕ = rsinΘ_y and h = rcosΘ, where Θ_x = arcsin (x'/r) and Θ_y = arcsin (y'/r) are the $\angle$'s between the x' = 0 and y' = 0 planes and the range vector r measured in the planes containing r. Subscript zero denotes the boresight direction, and $\Delta\Theta_x$, $\Delta\Theta_y$ are the angular deviations in the rx and ry planes from boresight.**

Since $h = r\cos\Theta_o$, the angular displacements are expressible in terms of the rectenna coordinates from foregoing relations as:

$$\Delta\Theta_x, \Delta\Theta_y \cong (x/h)\cos\Theta_o\cos\Theta_{xo}, (y/h)\cos\Theta_o\cos\Theta_{yo}.$$

Since, moreover, in the absence of grating lobes the beam is confined to small angular deviations,

$$\Psi_x \cong k\ell\Delta\Theta_x\cos\Theta_{xo} \cong \frac{2\pi x D_t \cos\Theta_o \cos^2\Theta_{xo}}{\lambda h N},$$

$$\Psi_y \cong k\ell\Delta\Theta_y\cos\Theta_{yo} \cong \frac{2\pi y D_t \cos\Theta_o \cos^2\Theta_{yo}}{\lambda h N}.$$

We can therefore write the intensity distribution on the rectenna in the more convenient form:

$$\frac{I(\hat{x},\hat{y})}{I_o} = \left\{\frac{\sin\frac{\pi\hat{x}}{2}}{N\sin\frac{\pi\hat{x}}{2N}}\right\}^2 \times \left\{\frac{\sin\frac{\pi\hat{y}}{2}}{N\sin\frac{\pi\hat{y}}{2N}}\right\}^2,$$

where

$$\hat{x} = \frac{x}{(\lambda h)/(2D_t\cos\Theta_o\cos^2\Theta_{xo})},$$

$$\hat{y} = \frac{y}{(\lambda h)/(2D_t \cos\Theta_o \cos^2\Theta_{yo})}$$

are dimensionless rectenna coordinates containing diffraction and incidence angle effects.

The utility of this transformation is that I/I_o distribution is now expressed as a universal function of the dimensionless coordinates $(\hat{x},\hat{y})$. Figure 7, for example, shows this phased array intensity distribution over the rectenna in the $\hat{y} = 0$ plane. (The distribution becomes independent of the number of elements when N is large enough to avoid grating lobes.) The nulls at $\hat{x} = \pm 2, 4,...$ define the boundaries of low-intensity sidelobes produced away from the main lobe. To compute the transmission efficiency, we approximate the phased array illumination pattern by the two dimensional Gaussian distribution,

$$\frac{I(\hat{x},\hat{y})}{I_o} \cong exp(-\hat{x}^2) \times exp(-\hat{y}^2),$$

whose spatial integrals can be expressed as error functions. As shown in Fig. 7, this 2D Gaussian is a close approximation to the phased array formula over the central zone where beam power is concentrated.

We find power incident on the rectenna P_r by integrating the 2D intensity distribution over an area element $dxdy$ between the rectenna edges at $x = \pm D_r/2$ and $y = \pm D_r/2$. The result is expressible in terms of the scan angles and a *powerlink parameter*, $\chi \equiv (D_t D_r)/(\lambda h)$:

$$P_r = \pi I_o \left\{\frac{D_r}{\chi \cos\Theta_o \cos\Theta_{xo} \cos\Theta_{yo}}\right\}^2 erf(\chi \cos\Theta_o \cos^2\Theta_{xo}) \times erf(\chi \cos\Theta_o \cos^2\Theta_{yo}).$$

where the error function here is defined[35]:

$$erf(z) \equiv \frac{2}{\sqrt{\pi}} \int_0^z exp(-t^2)\, dt .$$

A rational approximation for the error function given in Ref. 35 is used in our computer code. Since erf $(\infty) = 1$, the total transmitted power incident on an infinite rectenna is

$$P_t = \pi I_o \left\{\frac{\lambda h}{D_t \cos\Theta_o \cos\Theta_{xo} \cos\Theta_{yo}}\right\}^2,$$

which defines I_o in terms of the transmitted power, wavelength, altitude, transmitter aperture and the scan angles. A finite rectenna sees the same central intensity only intercepts a fraction of the transmitted power. This fraction is the instantaneous *transmission efficiency*:

$$\eta_t \equiv P_r/P_t = erf(\chi \cos\Theta_o \cos^2\Theta_{xo}) \times erf(\chi \cos\Theta_o \cos^2\Theta_{yo}).$$

It can be shown that $\eta_t(\chi, \Theta_o, \phi_o)$ has a weak periodic variation with ϕ_o over the four quadrants owing to the square aperture geometries. The azimuth-dependence vanishes entirely for circular apertures by symmetry and we neglect henceforth; evaluating η_t at $\phi_o = 0$. Figure 8 shows transmission efficiency in terms of the powerlink parameter for a range of zenith angles for zero azimuth. These results permit a preliminary sizing of the system. We want obviously to operate MTL at as high an η_t as possible given the other constraints on the system.

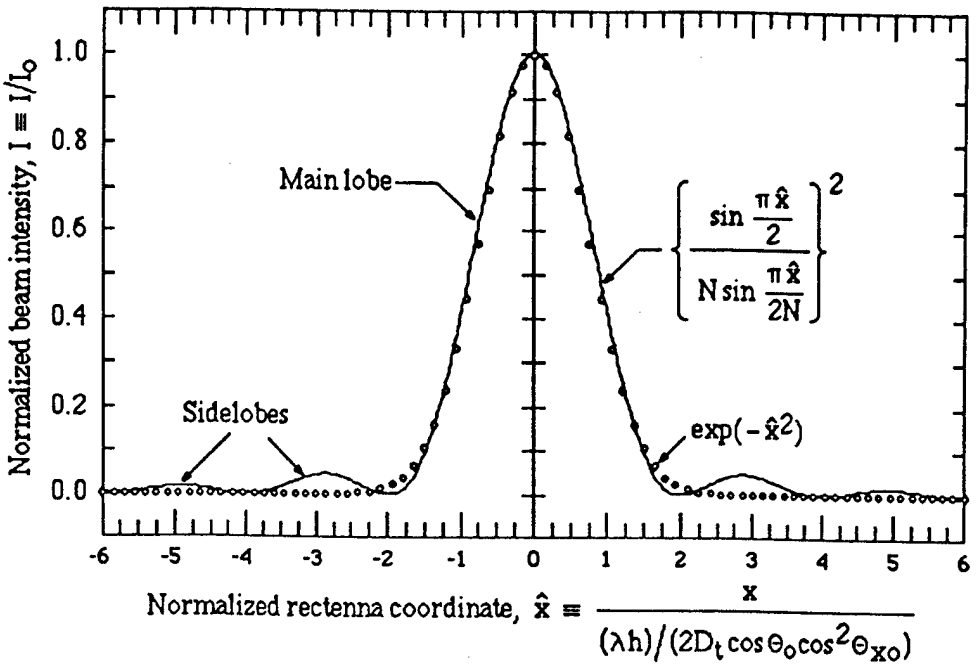

Figure 7. Dimensionless intensity distribution versus dimensionless x-coordinate along the rectenna at y = 0 from the phased array model compared with a Gaussian beam.

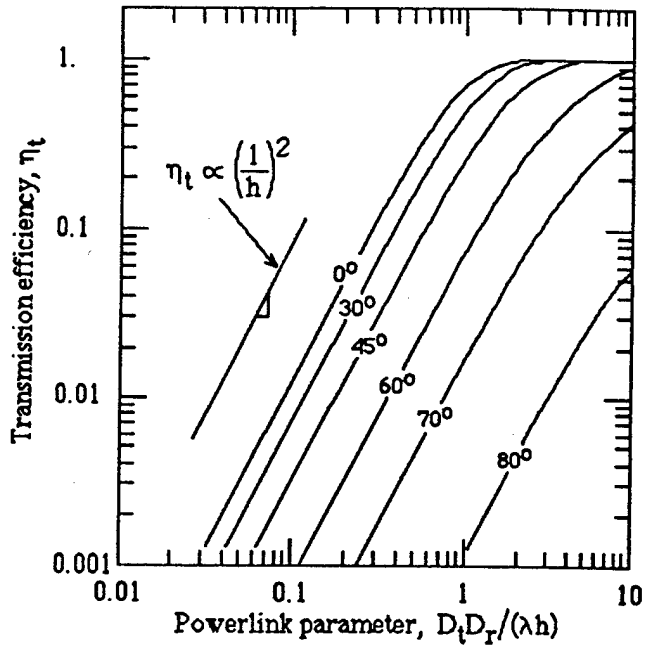

Figure 8. Transmission efficiency η_t of a Gaussian beam versus the powerlink parameter $\chi \equiv D_t D_r/(\lambda h)$ at $\phi_0 = 0$ for a range of zenith scan angles Θ_0 from overhead to 80°. At a given wavelength and scan angle, the transmission efficiency approaches 100% when $D_t \times D_r$ becomes very large, and decreases inversely with the square of altitude when $D_t \times D_r$ becomes very small. Acceptable efficiencies for MTL are produced when χ is of order unity .

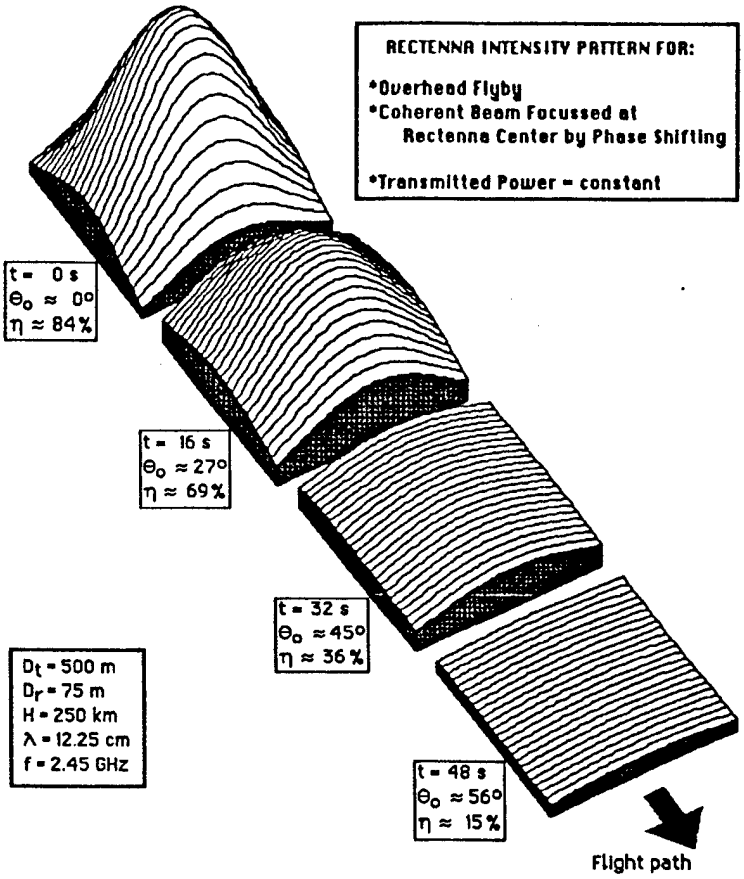

Figure 9. Distribution of incident beam intensity (power per unit area) in arbitrary units over the surface of a square horizontal rectenna as it overflies a phased array which points the beam at the rectenna center as it transmitting at constant power. A ground track is chosen for which $\Theta_{xo} = \Theta_0$ and $\Theta_{yo} = 0$. The full phased array formula was used, but the difference from the 2D Gaussian is small as the rectenna intercepts the intensity pattern in the main lobe.

As shown by the transmission efficiency curves plotted on logarithmic scales in Figure 8, for small powerlink parameters η_t scales with χ^2; or, all other parameters being constant, with the inverse square of altitude. On the other hand, transmission efficiencies approaching 100% are possible for a sufficiently large χ at the expense of large aperture products, small wavelengths or low attitudes, all of which which may be unacceptable for systems reasons. Once most of the beam main lobe power falls within the rectenna boundaries the return in efficiency of increasing χ reaches a point of diminishing returns. For preliminary sizing purposes, we adopt the criteria that $\chi^* \approx 1$ at some reference design point:

$$D_t^* = 500 \text{ m}, \; D_r^* = 100 \text{ m}, \; \lambda^* = 12.25 \text{ cm}, \; h^* = 408 \text{ km}.$$

The powerlink parameter for other apertures, wavelengths and altitudes is then given by

$$\chi = (D_t / D_t^*)(D_r / D_r^*)(\lambda^* / \lambda)(h^*/h)$$

The transmission efficiency computed above is valid instantaneously and varies over the flight path. A typical variation for an overhead flyby is shown in Figure 9 -- a 3D graphics rendering of the 2D intensity pattern on the surface of a square rectenna as it overflies the transmitter. The beam's projection on the horizontal rectenna spreads out in two dimensions, and the fraction of intercepted power decreases, as Θ_0 and range increase. Clearly, the instantaneous power transmission efficiency

peaks when the satellite is a minimum zenith angle. However, the total recoverable energy is the time integral of incident power between the peak scan angles, $-\Theta_{o,max} \leqq \Theta_o \leqq \Theta_{o,max}$.

If there were no limits on transmitted power levels, the best strategy to delivering a given total energy to orbit would be short, high power pulses at minimum zenith angle. However the conflicting objectives of minimizing thermal loads at the rectenna and transmitter, and of minimizing the electrochemical cell mass onboard the spacecraft -- which scales roughly with power level that must be accommodated -- drive the system in the opposite direction; to reduced power levels, longer transmissions and hence larger $\Theta_{o,max}$'s. A large $\Theta_{o,max}$ is also required to make large volume of sky accessible to the powerbeam transmissions of a given ground station, and may therefore be desirable despite the efficiency penalty . It may be more cost effective to compensate for the reduced η_t at high scan angles by transmitting at higher power levels than to build more ground stations and antennas with small $\Theta_{o,max}$'s, each of which sees fewer satellites.

To assess these issues, it is helpful to express the zenith scan angle of the beam in a plane containing the transmitter and rectenna in terms of the angle ψ between the zenith and a ray from the center of the Earth (Figure 11). So long as h << R_e the Θ_o of Figure 10 is 7mately equal to the polar coordinate Θ_o of Figure 8. From geometrical considerations then:

$$\tan \Theta_o = \frac{(R_e + h) \sin \psi}{h - (R_e + h)(1 - \cos \psi)} .$$

In the results presented in the next section we computed $\psi = \psi(\Theta_o, h)$, which is given implicitly by this equation, using a Newton-Raphson iteration subroutine.

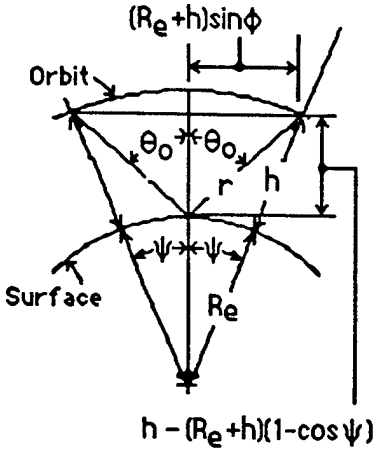

Figure 10 Angle geometry.

For low earth orbit scenarios, satellites are accessible to transmission over only a small fraction of their orbital periods (of order a few to ten percent). Let f be the fraction of the orbital period during which transmissions occur, and ψ_{max} be the angle measured from the Earth's center corresponding to the peak scan angle $\Theta_{o,max}$ measured from the Earth's surface. A circular orbit at altitude h in the plane of the transmitter is accessible to transmissions over the arc $2\psi_{max}$. If the transmitters are distributed such that they see each satellite once per orbit, the orbital accessibility fraction is $2\psi_{max}/(2\pi)$, or:

$$f(h, \Theta_{o,max}) = \frac{\psi_{max}}{\pi},$$

The time interval during which transmissions are possible is $\tau_t\,(h, \Theta_{o,max}) = f(h, \Theta_{o,max}) \times T(h)$, where T(h) is the orbital period. The time derivative of $\psi(t)$ is the component in the ground track plane of the satellite's angular velocity, so from the orbital mechanics we can find $\psi(t)$ and hence $\Theta_o(t)$ as functions of time. For systems analysis it is useful to work with a mean transmission efficiency $<\eta_t>$ and a mean scan angle $<\Theta_o>$ defined by:

$$<\eta_t\,(h, \Theta_{o,max})> \equiv \frac{1}{\tau_t} \int_{-\tau_t/2}^{\tau_t/2} \eta_t\,[\Theta_o(t)]\,dt \equiv \eta_t\,(h, <\Theta_o>).$$

Note also that Figure 11 can also be interpreted as a cross section through a latitude circle if R_e is replaced by $R_e \times cos(latitude)$ -- the distance from the Earth's axis to the surface -- and the arc of angular width $2\psi \equiv \Delta = \Delta(h, \Theta_{o,max})$ is interpreted as the longitude interval which can be viewed by each ground station along a latitude circle. This relation is used below to compute the number of ground stations N_g needed to see all satellites in near polar orbits at least once per orbit if they are uniformly distributed as a "picket fence" around a latitude semicircle: $N_g(h, \Theta_{o,max}) = \pi/\Delta$. Again a Newton-Raphson iteration is performed to compute N_g in terms of altitude and peak scan angle

6. HOUSEPEEPING POWER FROM ARCTIC PICKETS: AN MTL APPROACH

To illustrate the applicability of microwave power beam transmissions, we have considered a concrete system employing several land-based transmitters at Arctic latitudes designed to regenerate chemical energy for housekeeping power on a constellation of satellites in near polar orbits. The system looks attractive for several reasons, but it should be borne in mind that it is only one among many possible configurations utilizing the MTL concept. To preserve the widest options in orbital altitude, we assume all transmitters are steerable in both azimuth and zenith.

Orbits which are highly inclined relative to the Earth's equatorial plane are desirable for the SDI mission which requires satellites to be in range of ICBM deployment zones in the Eastern Hemisphere. With an orbital inclination of 90^o, a satellite passes over the North and South Poles sixteen times a day at a typical altitude of 300 km. For a spherical Earth, each time a polar-orbiting satellite crosses the equator, roughly every hour and a half, it does so 22.5^o further to the west than on the prior transit, although the actual precession may be influenced by the Earth's oblateness (see below). A single transmitter site at the North or South Pole would therefore see all satellites in polar orbit. However, there are geographical, geopolitical and mission considerations which argue for constellations in highly inclined, but not precisely polar, orbits. For example, the Earth's oblateness requires that at satellite at 300 km must have an orbital inclination of 97^o (so the highest latitude that it reaches is 83^o) in order to cross the equator at the same local time. Such so-called Sun-synchronous orbits are often used when it is particularly useful for some part of the surface to be visible from a satellite under the same conditions of solar illumination for extended periods of time[36]. In any event, it is reasonable to assume orbital planes of sufficient inclination that all satellites cross a 65^o N latitude circle twice each orbit (once each on their ascending and descending nodes). Accordingly, for any zenith angle range scannable from East to West by the transmitters, there is some minimum number of transmitters, N_g, uniformly spaced around a latitude semicircle, that see all satellites at least once per orbit. To minimize the stored mass of working gases cycling through the electrochemical cell, we have designed for at least one regenerative cycle, and therefore one orbital segment accessible to transmissions, per orbit.

As shown in Figure 11, there are at least seven potential sites on land in the Arctic for MTL transmitters uniformly spaced about 30^o apart along a 180^o longitude segment at 65 ^{o}N latitude. A more poleward latitude might require siting these in the Arctic ocean, while a more equatorward ring would permit access to fewer orbits per station. Without ruling out floating transmitters at lower latitudes, we believe seasonal sea ice packs in the Arctic ocean would impose unacceptable instabilities, maintenance problems and structural requirements on permanent transmission stations. In the southern hemisphere, the only solid surface available at high latitudes is atop the one kilometer ice sheet capping Antarctica, a climatically hostile terrain for a permanent station, and one also ringed by seasonal sea ice. The internationalization of the Antarctic continent may pose institutional barriers to near term deployment as well, although this might be addressable in the future by appropriate treaties.

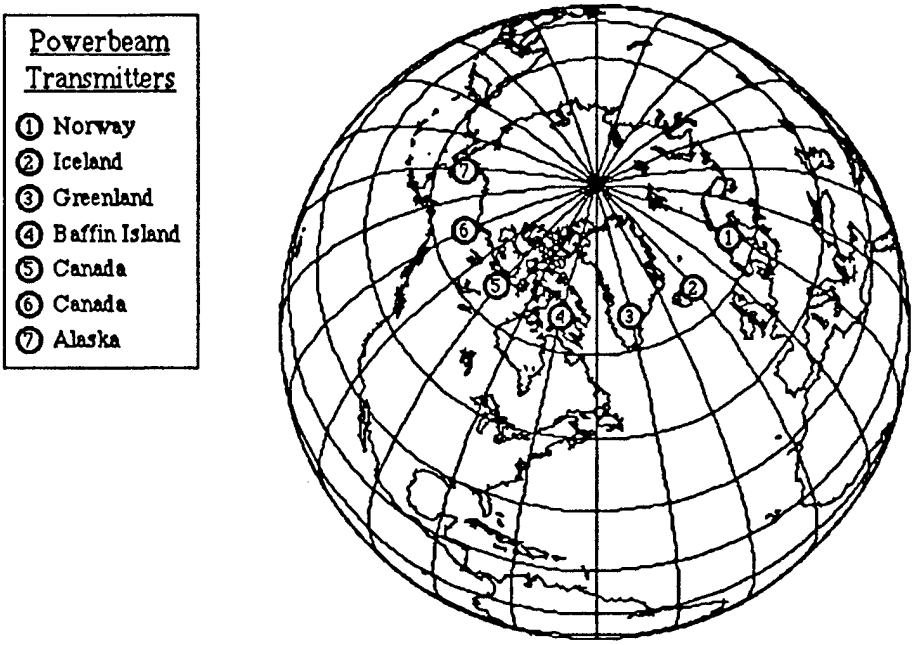

Figure 11. Potential land locations of Picket Fence stations deployed around an Arctic semicircle at 65 ^{0}N latitude, and spaced approximately 30^{0} apart in longitude, to recharge onboard electrochemical cells by surface transmissions of microwave beams. Satellites in near polar orbits above 250 km altitude are accessible to transmissions from one or more of these 7 ground stations at least once each orbit (Figure 12).

From the standpoint of accessibility, the number of stations needed is independent of the power levels of the transmissions. The transmitter power needed depends on the mean efficiency of transmission, the orbital accessibility and on the total energy required to regenerate the oxidizer and fuel from their product. Suppose the total energy received during transmission time τ_t is converted to housekeeping energy over the entire orbital period T with a system efficiency $\eta_{sys} = (P_H \times T)/(P_t \times \tau_t)$; where η_{sys} includes the efficiency of the rectenna in converting the incident wave to DC, dissipative losses in the power conditioning circuitry, and the "round trip" efficiency of the electrochemical cell (electrolysis efficiency × fuel cell efficiency). For conservation of energy, $P_H \times T = \eta_{sys} \times <\eta_t> \times P_t \times f \times T$; which can be solved for the required level of transmitted power,

$$P_t = \frac{P_H}{\eta_{sys} \times <\eta_t> \times f}.$$

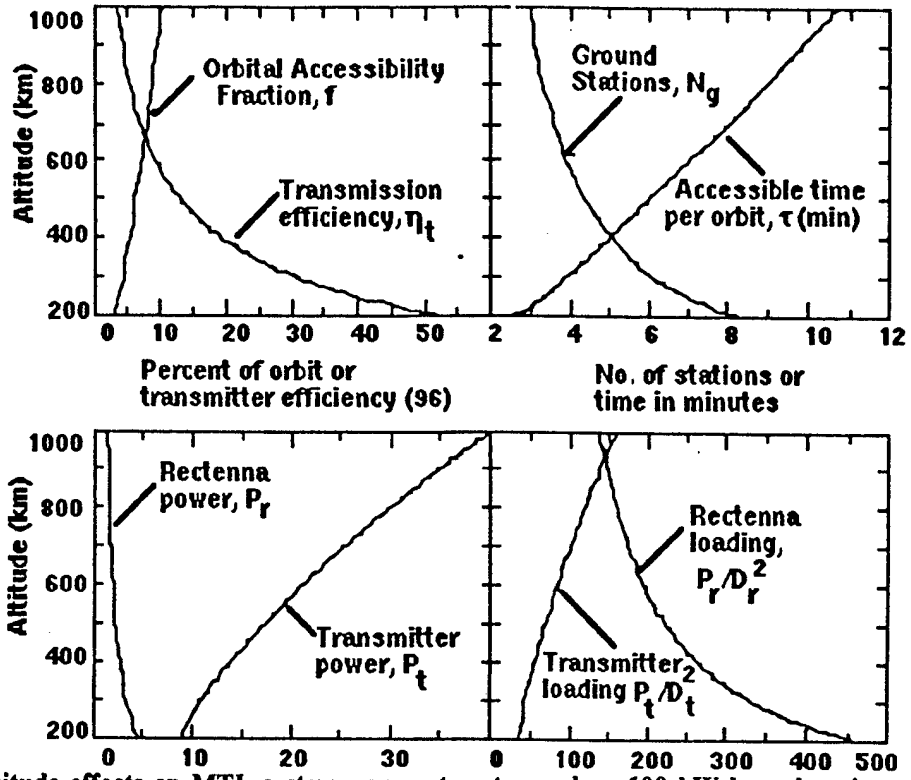

Figure 12. Altitude effects on MTL system parameters to produce 100 kW housekeeping power for satellites in near polar orbits. The land-based "picket fence" of phased array transmitters uniformly distributed around a 65° N latitude semicircle assumed in these calculations was constrained by the specifications: $\Theta_{o,max} = 75^o$, $\langle\Theta_o\rangle = 50^o$, $D_t = 500$ m, $D_r = 100$ m, $\lambda = 12.25$ cm (2.45 GHz) and $\eta_{sys} = 70\%$. (TOP LEFT) Accessibility fraction per orbit and transmission efficiency ($f, \langle\eta_t\rangle$) ; (TOP RIGHT) minimum number of ground sites needed to "see" all satellites at least once per orbit and accessible transmission time (N_g, τ_t); (BOTTOM LEFT) transmitted and received power (P_t, P_r) ; and (BOTTOM RIGHT) power loadings (P_t/D_t^2 , P_r/D_r^2)

The result is independent of the orbital period as such. For the specified level of housekeeping power, $P_H = 100$ kW, transmitter power needed depends inversely on the product of the mean transmission efficiency $\langle\eta_t\rangle$ and the orbital accessibility fraction f.

Figure 12 shows the altitude variation of key parameters for a reference system of MTL transmitters deployed around a latitude semicircle at 65° N as in Figure 11. For the given peak and mean scan angles, the accessible fraction of the orbit increases with altitude because transmitters see a larger segment of the satellite constellation shell. We chose relatively large scan angles to maximize the swept volume of space per station, and a powerlink parameter of order unity. Under these conditions, the decrease of mean transmission efficiency with altitude approaches the inverse square regime of Figure 8 ($\langle\eta_t\rangle \propto h^{-2}$). The minimum number of ground sites needed to see each satellite once per orbit N_g is less than the seven shown in Figure 11 for altitudes $\geq$ 250 km. Besides the accessibility requirement on sites, it is necessary to consider how many individual transmitters are needed to continuously beam power to a given number of satellites, since for very large numbers more than one may be in view at any given time. If N_{sat} is the total number of satellites, the number of individual transmitters needed to continuously charge each of them during the accessible part of their periods is $N_{sat} \times f$. For example, at 500 km altitude Table 2 shows $N_{sat} \approx 122$ defensive satellites for the nominal laser but only 52 for the "bright" laser. Since f (500 km) $\approx$ 6.25 % (from Figure 12) we need 8 individual transmitters for the nominal laser, but only 4 for the bright one. The seven ground stations of Figure 6 with one transmitter at each site could therefore service all defensive satellites with bright lasers at 500 km, although more more than one transmitters per site might be needed for the nominal laser brightness case.

In the lower panels of Figure 12 we show the altitude dependence of transmitted power and power incident at the receiver as well as the power loading of the receiver and transmitter. The transmitter power required increases with increasing altitude because efficiency decreases, but this is mitigated to some extent by the the increased accessibility fraction at higher altitudes which allows energy needed over the orbit to be delivered at lower rectenna power levels. At the transmitter end of the link aperture powers of 10-40 MW are needed corresponding to power loadings of 40 - 160 W m^{-2}. Because of transmission losses the rectennae see lower incident power, but because this power is focussed on smaller apertures their power loading is higher than the transmitter's below about 950 km.

While no phased array transmitters have been constructed yet for direct power transmissions to spacecraft, many major technological issues associated with power beams have been addressed in phased arrays for radar surveillance and tracking of missiles and satellites. Table 4, for example, gives salient characteristics of the US Cobra Dane radar -- a 30 meter phased array in Shemya, Alaska. The Soviet Union too recently unveiled a massive 11 story high phased array transmitter under construction at Krasnoyarsk, Siberia, and thought to operate at frequencies $\leq$ 0.2 GHz (Ref. 37). (The northward orientation of this radar is controversial since it suggests it may be a component of an anti ballistic missile system, a possible violation of the present ABM treaty.)

Table 4. Specifications of the COBRA DANE radar transmitter (AN/FPS- 108): A two-axis phased array (Ref. 38).

Type	Multifunction array for search and track of missiles and satellites
Manufacturer	Raytheon
Location	Shemya, Alaska
Frequency band	L-band
Frequency (GHz)	1.215-1.250 (NB); 1.175-1.375 (WB)
Power, peak (MW)	15.4
, mean (MW)	0.92
Antenna aperture (m)	29
Beam shape	Pencil
Type scanner	Phase-Phase
Angular scan coverage, zenith (deg)	$\pm$ 60° (NB), $\pm$ 22° (WB)
, azimuth (deg)	$\pm$ 60° (NB), $\pm$ 22° (WB)
Pulse width, transmit (μs)	150-1500; 2000; 1000; 1000
Tube type	96 TWT's

In any event, the design and operation of high power transmitters in Arctic locales can be considered a near state-of-the art technology, although scale-up to 500 meter apertures is admittedly a major engineering challenge, particularly as regards cost minimization (see below). Electronically, the main difference between phased array radars and MTL transmitters is that for radar beams power is typically transmitted in high power millisecond pulses to provide discernable echo returns, whereas the continuous (cw) beams proposed here are designed for relatively uniform power levels at satellite rectennae.

The mean power level of Cobra Dane of 0.92 MW corresponds to a transmitter power loading $\sim$ 1000 W m^{-2}. This is about 17 times less than peak levels attained during pulses. Nonetheless, Cobra Dane's mean intensity is still an order of magnitude larger than the transmitter power loadings of our reference MTL system. The environmental impact of microwave radiation from our reference system's beams on local ecosystems (including man) would be substantially below presently operational radars. While standards vary in different countries, occupational exposure limits to continuous microwave radiation are generally in the range of 10-100 W m^{-2} (Ref. 14). The beam intensity at the periphery of the transmitter from sidelobe radiation would be substantially below these values. Even the occasional flight of migratory birds through the beam should experience few ill effects.

A potentially deleterious effect of high beam intensities at the rectenna is rectenna diode heating by prompt thermal dissipation[28]. However, it is easy to show that dissipative heating effects would be small for the rectenna power loadings of Figure 12 if heat can be conveyed away from the diodes to the rectenna surface sufficiently rapidly. If all the incident microwave power is absorbed by the rectenna, the dissipation rate per unit area is $Q_{diss} \approx (P_r/D_r^2) - Q_{store}$, where Q_{store}

is the sum of chemical and thermal storage rates per unit rectenna area during charging. (This stored energy is released over the orbit as a whole at reduced rates of order $f \times Q_{store}$.) The rectenna temperature T_r when the beam is on is then governed by the energy balance: $Q_{sun} + Q_{earth} + Q_{diss} = Q_{loss}$, where Q_{sun} is the absorbed solar flux, Q_{earth} is the absorbed infrared flux from the Earth, and $Q_{loss} \approx 2\sigma T_r^4$ is the radiative cooling per unit area from both sides of a unit emissivity rectenna with $\sigma = 5.67\ 10^{-8}$ W m^{-2} K^{-4} the Stefan Boltzmann constant. Under "worst case" conditions where the full solar constant is absorbed (Q_{sun} = 1360 W m^{-2}), all terrestrial infrared flux is absorbed (Q_{earth} = 240 W m^{-2}), and 30% of the peak rectenna power loading is dissipated promptly (Q_{diss} = 150 W m^{-2}), Q_{loss} = 1750 W m^{-2} and $T_r = [Q_{loss}/(2\sigma)]^{1/4}$ = 352 K. This is only 7 K warmer than when the beam is off because the prompt dissipation of microwave power is a small component of the total heat flux. A thermal engineering approach to minimizing the diode temperature T_d is therefore to construct thermal busses between diodes and the rectenna surface of sufficiently high conductance that dissipation to space from the rectenna area as a whole is rate-limiting to diode cooling. In any case, gallium arsenide diodes can operate at $T_d \leqq$ 450 K while still providing good lifetimes[28], so diode heating should not be a serious problem.

Besides beam transmission and reception, thermal management, deployment, and environmental issues, it is necessary to consider whether reliable and relatively lightweight storage and interconversion of electrical and chemical energy over many charge-discharge cycles -- a requirement of the system -- can be produced by near state-of-the-art technology. A detailed analysis of onboard energy conversion systems for MTL will be given in a forthcoming publication, but a brief discussion is in order here. Both batteries and fuel cells convert chemical energy of reduction-oxidation (redox) reactions to electrical energy. Both employ positive electrodes (anodes) and negative electrodes (cathodes) separated by an electrolyte solution or solid matrix through which an ionic current flows. Regenerative fuels cells (which can also be run "backwards" as electrolyzers) differ from batteries insofar as reactants are stored outside the cell. By pumping reactants through the cell at high flowrates, efficient high power density operation is possible, provided dissipative losses due to electrical resistance in the electrolyte and contacts, and polarization effects, can be minimized. For space applications, it is desirable to employ redox reactions which provide a high free energy change per unit mass; e.g, $H_2 + (1/2)O_2 \rightleftharpoons H_2O$. Table 5 summarizes properties of five cell types characterized by their electrolyte. These determine the ion type migrating across the electrodes. Electrons too are produced at the electrodes, and provide the charge balance between currents flowing though the internal and external circuits.

Table 5. Comparison of electrochemical cell technologies for onboard space power(Refs. 39, 40)

Type	Alkaline	Solid Polymer	Phosphoric Acid	Molten Carbonate	Solid Oxide
Electrolyte	KOH	Nafion	H_3PO_4	(Li, K)CO_3	$Zr(Y)O_2$
Migrating ion	OH^-	H^+	H^+	CO_3^{-2}	O^{-2}
Temperature (K)	350	350	270	920	1270
Coolant channel	inert loop	inert loop	inert loop	reactant gas	reactant gas
Largest size tested (kW)	32	5	4,500	2	5
Reversible operation ?	separate stack	separate stack	no	no	same stack
Power density, Cell only (kW kg^{-1})	4.0	0.28	0.1	0.1	15.0

The cell with the greatest potential for high power density we want for MTL housekeeping has solid oxide ceramic electrolytes. These have the additional desirable properties of reversible operation and employing reacting gases for cooling. To get high efficiencies, of order of 80-90%, solid oxide cells must operate at sufficiently high temperatures (1200-1300 K)

that the ionic resistivity of zirconium oxide becomes appropriately small. A so-called monolithic solid oxide fuel cell composed of adjacent triangular cross-section channels of integrated ceramic electrodes and electrolyte through which pressurized oxygen, hydrogen and steam flow is under development at Argonne National Laboratories. Fee et al.[39,40] have proposed such monolithic cells driven by nuclear reactors for the SDI burst mode power (Figures 1 and 2). Such a unit would require a significant scale-up to the 100 MW power level from the 5 kW achieved in the laboratory thus far but the basic principles have already been demonstrated. In the Argonne design, the reactor is used to regenerate oxygen and and hydrogen from steam subsequent to pulsed power discharges for further pulses in order to reduce the mass of reactants carried to orbit. But if the cell is limited to a given power density in both electrolysis and fuel cell modes, it is not clear why the nuclear reactor power is not used directly. The advantage, indeed the necessity, of a reversible electrochemical cell is clear for MTL where electrical energy is available only during a small fraction fraction of the orbit and must be regenerated over the entire orbit.

Interestingly, the Argonne monolithic fuel cell originally proposed for nuclear pumped burst mode power is directly applicable to our proposed MTL housekeeping application in the somewhat more modest proportions of a 5 MW unit -- the level of peak received power at 200 km in the picket fence system of Figure 13. At a power density of 10 kW kg^{-1}, the cell would have a mass of only 500 kg, to which of course the mass of fuel, oxidizer and tank would have to be added. We estimate these in the range of 2000-4000 kg. This seems a very modest mass penalty to pay to generate housekeeping power for satellite constellations by entirely non-nuclear means. If sufficient chemical fuel could be brought to orbit to provide burst mode power as well, or as has been suggested[4], if the directed energy weapons remained on the ground and defensive satellites were essentially mirrors requiring only housekeeping power, then the possibly would seem to exist for an SDI defense with no need for orbiting nuclear materials.

7. EFFECTS OF INCLINED ORBITS AND NON-OVERHEAD PASSES ON MTL.

In Section 6, the satellite constellation was assumed to be in polar orbit (i.e the inclination of the satellite's orbital plane is 90° with respect to the equatorial plane) and only overhead passes over the transmitting antenna were considered (in estimating the system parameters and performance). Here we investigate the effects of non-polar orbits and non-overhead passes on the system.Since the rectenna size is a major constraint and cost driver, the analysis has focussed on linking the other parameters to the rectenna size.In orbit, the satellite will trace out an ellipse in inertial space while the earth turns beneath it. A particular choice of orbit / transmitting station locations will affect the MTL system through the geometry of the transmitter-satellite link.The number of possibilities is large but are constrained by the spatial distribution of the constellation, the location of the boosters and, in our case the location of the transmitting stations.An overhead pass over a transmitter has a larger accessibility fraction as compared to a non-overhead pass.

The choice of orbit inclinations has been investigated by a number of investigators including Bloembergen and Patel[4].Since the Soviet land mass and existing missile fields are at relatively high latitudes (~ 57°) orbits with an inclination of 57° will give the maximum coverage of the boosters.It would therefore be advantageous to locate the transmitting stations at this latitude.The case we considered in our earlier study was that of Polar orbits and overhead passes over an Arctic picket fence of transmitters (~ 65° N lat).To properly investigate the effects of inclined orbits on the size of microwave receiving antenna, a statistical study should be undertaken. An orbital dynamics program should be run for many orbits, and thus the power received by a rectenna of a given size, can be calculated(since the power received is a function of both the availability of the satellite and the instantaneous angles between the satellite and the ground station). Such a study is well beyond our current program plan.

As an approximation, we have run our orbital dynamics program for a simulated 24 hour period with the provision that the 24 hour period include at least one nearly overhead pass (zenith angle > 85 degrees). In our model, we fixed the transmitter power at 40 Megawatts, the maximum scan angle at 30 degrees from the horizon, and the received power was specified to be sufficient to provide 100 kw to the spacecraft over the balance of the time(assuming an overall microwave to dc and fuel cell efficiency of 43%).In the graph below, we present the results of this calculation.

For comparison, a curve is shown for the polar orbit case, where the polar orbit corresponds to the best case scenario, at the same time the inclined case has oblique passes averaged in with overhead passes(and therefore the rectenna size is larger than for the strictly overhead case).

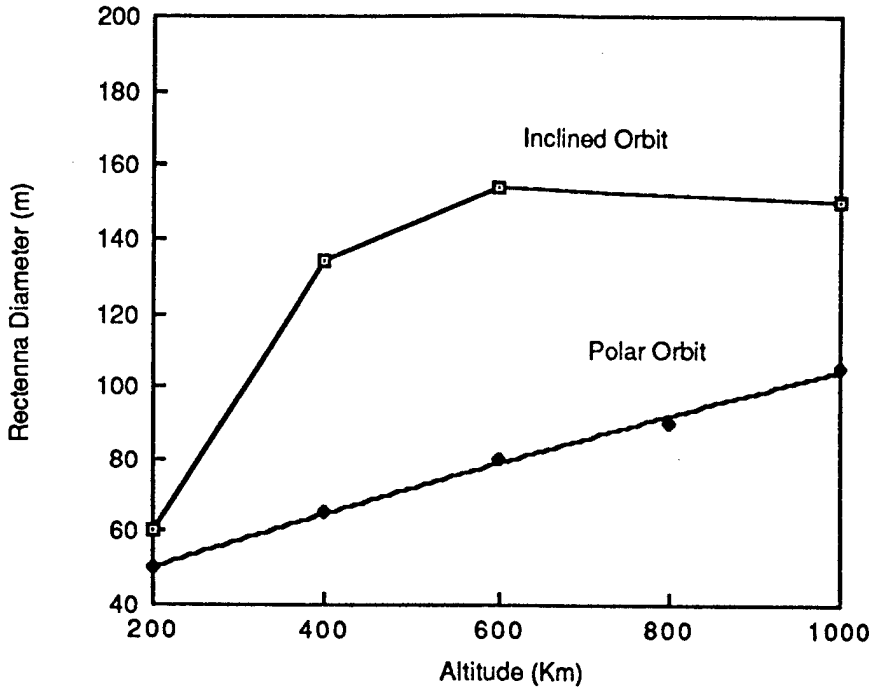

Figure 13. Effects of inclined orbits and non-overhead passes on MTL system . The orbit inclination used was 70^0 , the transmitting stations were situated at 65^0 N latitude , the other parameters were fixed at $\Theta_{o,max} = 60^0$ $D_t = 500$ m, $\lambda = 12.25$ cm (2.45 GHz) and $\eta_{sys} = 43\%$.

The optimum case (corresponding to that satisfying the booster requirement and that of the transmitting antenna location) will lie between the two cases shown here. In addition, the earth's equatorial bulge produces a torque which causes inclined orbits to drift in longitude. It is clear therefore that two axis tracking will be necessary, since the spacecraft rarely repeats the same ground track over a transmitter site, and the effect of this on cost must be examined..

8. ACKNOWLEDGEMENTS

We thank William C. Brown, inventor of the rectenna and SPS pioneer, and Darrell C. Fee, manager of the Solid Oxide Fuel Cell Program at Argonne National Laboratory, for their valuable contributions to this study. This research was sponsored by the Strategic Defense Initiative Organization (under contract DAAL02-86-K-0116) Office of Innovative Science and Technology, and managed by Dr. Howard Brandt of the Harry Diamond Laboratories,

9. REFERENCES

1) Fletcher, J.C., "The Strategic Defense Initiative: Defensive Technologies Study," Department of Defense, Washington, DC, April 1984; available from U.S. Government Printing Office, Washington, DC, April 1984.
2) Carter, A.B., "Directed Energy Missile Defense in Space," U.S. Congress, Office of Technology Assessment, Washington, DC; available from U.S. Government Printing Office, DC, April 1984.
3) Tirman, J. (Ed.), The Fallacy of Star Wars; based on studies conducted by the Union of Concerned Scientists, Vintage Books, 1984.
4) Bloembergen, N. and C.K. Patel (Eds.) Science and Technology of Directed Energy Weapons. American Physical Society, New York, 1987; to appear in Reviews of Modern Physics.
5) Sholtis, J.A. (1987) "Programmatic, Technical, and Safety Overview of the SP-100 Space Reactor Power Program," Presented at the 3rd SDI Workshop on Space Experimentation, Orlando, Florida, June 2-4, 1987; available from SP-100 Program Office, Air Force Element, Dept. of Energy, DEP/NE-521 (GTN), Washington, DC.
6) Salisbury, D.F., "Radiation Risk and Planetary Exploration," Planetary Report, Vol. 7, No. 3, 1987, pp. 3-7.
7) Glaser, P.E., "Power from the Sun: Its Future," Science, Vol. 162, Nov. 1968, pp. 857-861.
8) Brown, W.C., "The Technology and Application of Free-Space Power Transmission by Microwave Beam." Proceedings of the IEEE, Vol. 62, No. 1, January, 1974, pp. 11-25
9) "Preliminary Environmental Assessment for the Satellite Power System," Document DOE/ER-0036, Office of Energy Research, U.S. Department of Energy, Washington, DC, 1975.
10) Kraft, C.C., Jr., "The Solar Power Satellite Concept--The Past Decade and the Next Decade". Von Karman Lecture, 15 Annual Meeting of the AIAA, Washington, DC, Feb. 6-9, 1979; AIAA Preprint 79-0534, American Institute of Aeronautics and Astronautics, 1290 Avenue of the Americas, New York, NY 10019.
11) Schwenk, F.C. (1983) "Summary Assessment of the Satellite Power System," Journal of Energy, Vol. 7, No. 3, May-June 1983, pp. 193-199.
12) Ericke, K.A., "The Power Relay Satellite: A Means of Global Energy Transmission through Space," Internal Document, North American Space Operations Center, Rockwell International Corporation, El Segundo, CA, 1973.
13) Rogers, T.F., "Reflector Satellites for Solar Power," IEEE Spectrum, Vol. 18, No. 7, 1981, pp. 38-43.
14) "Electric Power From Orbit: A Critique of a Satellite Power System," National Academy of Sciences, Washington, DC, June 1981.
15) Brown, W.C. and Glaser. P.E., "An Electric Propulsion Transportation System from Low-Earth Orbit to Geostationary Orbit Utilizing Beamed Microwave Power," Space Solar Power Review, Vol. 4, 1983, pp. 119-129
16) Forward, R.W., "Starwisp: An Ultra-Light Interstellar Probe," Journal of Spacecraft and Rockets, Vol. 22, No. 3, 1984, pp. 345-350.
17) Culp, A.W. , Jr., Principles of Energy Conversion. McGraw-Hill, New York, 1979.
18) Salkeld, R., Patterson, D.W., and Grey, J., Space Transportation Systems. American Institute of Aeronautics and Astronautics, New York, NY, 1978.
19) Joels, K.M., Kennedy, G.P., and Larkin, D., The Space Shuttle Operator's Manual. Ballantine Books, NY, 1982.
20) "Space Station Reference Configuration Description." Document JSC-19989, August, NASA Johnson Space Center, Houston, TX, 1984.
21) Field, G. and Spergel, D., "Cost of Space-Based Laser Ballistic Missile Defense," Science, Vol. 231, 1986, pp. 1387-1393.
22) Hoffert, M.I. and Miller, G., "Ballistic Missile Defense: Cost of Space-Based Laser," Science, Vol. 234, Nov. 1986, pp. 1057-1059.
23) Bate, R.R., Mueller, D.D., and White, J.E., Fundamentals of Astrodynamics, Dover Publications, New York, 1971.

24) Goetz, A.F.H. and Rowan, L.C., "Geologic Remote Sensing," Science, Vol. 211, 1981, pp. 781-792.
25) Brown, W.C., "Design Study for a Ground Microwave Power Transmission System for Use with a High Altitude Platform," Final Report PT-6052, 1982, Raytheon Company, Power Tube Division, Waltham, Massachusetts.
26) Goubau, G., "Microwave Power Transmission from an Orbiting Solar Power Station," Journal of Microwave Power, Vol. 5, No. 4, 1970, pp.223- 231.
27) Brown, W.C., "Electronic Components for Microwave Power Engineering," Electronic Progress, Vol. IX, No. 4, 1965, pp. 9-13, Ratheon Corporation, Lexington, MA.
28) Brown, W.C., "Earth to Space DC to DC Power Transmission System Utilizing a Microwave Beam as a Source of Energy for Electric Propelled Interorbital Vehicles," Presented at AIAA Electric Propulsion Conference, Sept. 30-Oct. 2, 1985, Alexandria, VA.
29) Glaser, P.E., "Microwave Power Transmission for Use in Space," Microwave Journal, December, 1986, pp. 44-58.
30) Durnin, J., Micelli, J.J., Jr. and Eberly, J.H., "Diffraction Free Beams", Physical Review Letters, Vol. 38, No. 15, 1987, pp. 1499- 1501.
31) Born, M. and Wolf, E., Principles of Optics, Sixth edition, Pergamon Press, NY, 1980, pp. 392-401
32) Tang, R. and Burns, R.W., "Phased Arrays" in Antenna Engineering Handbook, edited by R.C. Johnson and H. Jasik, Chapter 25, McGraw-Hill, NY, 1984.
33) Skolnik, M.I., Introduction to Radar Systems, 2nd Edition, McGraw-Hill, NY, 1980.
34) Balanis, C.A., Antenna Theory: Analysis and Design. Harper and Row, NY, 1982
35) Abramowitz, M. and Stegun, I.A., Handbook of Mathematical Functions, Dover Publications, Inc., NY, 1970.
36) Shapland, D. and Rycroft, M., Spacelab: Research in Earth Orbit, Cambridge University Press, NY, 1984
37) Broad, W.J., "Soviet Radar on Display", New York Times, Sept. 9, 1987, p. A1.
38) Brookner, E. (Ed.), Radar Technology, Artech House, 610 Washington St., Dedham, MA, 1977.
39) Fee, D.C., and 14 co-authors, "Fuel Cell Development for SDI Applications," August 1986, Chemical Technology Division, Argonne National Laboratory, Argonne, Illinois.
40) Fee, D.C., and 14 co-authors, "Multimegawatt Space Nuclear Power," Annual Report on Monolithic Fuel Cell Technology Development, Sept. 1986, Chemical Technology Division, Argonne National Laboratory, Argonne, Illinois.